



Monolithic anion-exchange chromatography yields rhinovirus of high purity



Günter Allmaier^a, Dieter Blaas^b, Christina Bliem^a, Thomas Dechat^b, Sofiya Fedosyuk^b,
Irene Gösler^b, Heinrich Kowalski^b, Victor U. Weiss^{a,*}

^a Institute of Chemical Technologies and Analytics, TU Wien (Vienna University of Technology), Vienna, Austria

^b Department of Medical Biochemistry, Medical University of Vienna, Vienna Biocenter, Vienna, Austria

ARTICLE INFO

Keywords:

Anion-exchange chromatography

Purification

nES GEMMA

RV-A2

Mass spectrometry

ABSTRACT

For vaccine development, 3D-structure determination, direct fluorescent labelling, and numerous other studies, homogeneous virus preparations of high purity are essential. Working with human rhinoviruses (RVs), members of the picornavirus family and the main cause of generally mild respiratory infections, we noticed that our routine preparations appeared highly pure on analysis by sodium dodecyl sulfate polyacrylamide gel electrophoresis (SDS-PAGE), exclusively showing the four viral capsid proteins (VPs). However, the preparations turned out to contain substantial amounts of contaminating material when analyzed by orthogonal analytical methods including capillary zone electrophoresis, nano electrospray gas-phase electrophoretic mobility molecular analysis (nES GEMMA), and negative stain transmission electron microscopy (TEM). Because these latter analyses are not routine to many laboratories, the above contaminations might remain unnoticed and skew experimental results. By using human rhinovirus serotype A2 (RV-A2) as example we report monolithic anion-exchange chromatography (AEX) as a last polishing step in the purification and demonstrate that it yields infective, highly pure, virus (RV-A2 in the respective fractions was confirmed by peptide mass fingerprinting) devoid of foreign material as judged by the above criteria.

1. Introduction

Picornaviruses are icosahedral particles of 30 nm diameter with a single-stranded (+) RNA genome enclosed within a non-enveloped protein shell composed of 60 copies each of the four capsid proteins VP1 through VP4. Physicochemical and structural analyses require sizable quantities of these viruses at high purity. Virus is usually recovered from infected tissue culture cells via lysis and purified by differential centrifugation followed by ultracentrifugation on sucrose, potassium tartrate, Nycodenz, or cesium chloride density gradients (e.g. references (Ashley and Caul, 1982; Gugerli, 1984; Liu et al., 2011)). Virus particles are recovered from selected fractions, pelleted, and resuspended in a suitable buffer. Working with RVs, which belong to the genus *Enteroviruses*, and cause more than 50% of all (mostly mild) respiratory infections, we noticed that routine preparations showed exclusively the four viral capsid proteins (VPs) upon sodium dodecyl sulfate polyacrylamide gel electrophoresis (SDS-PAGE). However,

Kremser et al. (Kremser et al., 2006) already demonstrated, by using capillary electrophoresis with UV absorbance detection (CE-UV) that RV-A2 purified via ultracentrifugation on a sucrose density gradient contained some additional material ('contaminant'). This material showed up as peak monitored at 200 nm UV absorption (typical wavelength for RV-A2 analysis applied in CE separation) in CE runs in presence of SDS above its critical micellar concentration in the background electrolyte (Kremser et al., 2006). Nevertheless, due to the low absorbance of this contaminant in relation to the virus, it was considered negligible for most experiments. However, when labelling RV-A2 with amine-reactive NHS-ester dyes, the contaminant became strongly fluorescent as seen in CE with laser induced fluorescence detection (CE-LIF), suggesting either the presence of many primary amino groups or non-covalent attachment of the dye to hydrophobic surface patches or pockets of the contaminant (Kolivoska et al., 2007; Kremser et al., 2004; Weiss et al., 2007).

Analysis of these RV-A2 preparations by negative-stain transmission

Abbreviations: ACN, acetonitrile; AEX, anion-exchange chromatography; CE, capillary electrophoresis; DTT, dithiothreitol; EDTA, ethylenediaminetetraacetic acid; EM, electrophoretic mobility; FCS, fetal calf serum; GEMMA, gas-phase electrophoretic mobility molecular analyzer; RV, human rhinovirus; RV-A2, RV-B14, RV-A16, RV-A89, RV serotypes; LIF, laser induced fluorescence; MALDI, matrix-assisted laser desorption ionization; MEM, minimal essential medium; MS, mass spectrometry; MOI, multiplicity of infection; nES, nano electrospray; PAGE, polyacrylamide gel electrophoresis; PMF, peptide mass fingerprint; PSD, post-source decay; SDS, sodium dodecyl sulfate; SMEM, spinner minimum essential medium; TCID₅₀, tissue culture infectious dose 50; TEM, transmission electron microscopy; TFA, trifluoroacetic acid; VP, viral protein

☆Note: Authors in alphabetical order.

* Corresponding author at: Institute of Chemical Technologies and Analytics, TU Wien (Vienna University of Technology), Getreidemarkt 9/164, A-1060 Vienna, Austria.

E-mail address: victor.weiss@tuwien.ac.at (V.U. Weiss).

<http://dx.doi.org/10.1016/j.jviromet.2017.09.027>

Received 7 July 2017; Received in revised form 27 September 2017; Accepted 27 September 2017

Available online 28 September 2017

0166-0934/ © 2017 The Authors. Published by Elsevier B.V. This is an open access article under the CC BY license (<http://creativecommons.org/licenses/by/4.0/>).

electron microscopy (TEM) revealed cloud- or ‘popcorn’-shaped amorphous masses (Bilek et al., 2009). By the same token, analysis by means of a nano Electrospray Gas-phase Electrophoretic Mobility Molecular Analyzer (nES GEMMA) (Kaufman et al., 1996) revealed the presence of two similarly-sized components (Bacher et al., 2001); the virus gave a sharp, and the second component a very broad peak indicating polydisperse particles (Weiss et al., 2012). Both sample components shared similar apices at about 30 nm dry particle diameter.

nES GEMMA separates single-charged nanoobjects obtained from a nES process with subsequent charge reduction in a bipolar atmosphere induced by a ^{210}Po α -particle source or a soft X-ray beam in the gas-phase at ambient pressure. The analytes become separated according to their electrophoretic mobility (EM) diameter in a tunable electric field and an orthogonal constant laminar high-sheath flow of particle-free air. Only particles of a given EM diameter (corresponding to the dry particle size in case of spherical analytes) can pass the size analyzer at a given voltage. The latter is varied to scan a predetermined size range. Detection is based on scattering of a laser beam focused on the separated, monodisperse analytes that create droplets in the supersaturated *n*-butanol or water atmosphere of the detector unit. Thus, particle counting is independent of their chemical nature resulting in number-particle concentrations, as suggested by the European Commission for nanoparticle characterization (2011/696/EU from October 18th, 2011). nES GEMMA has proven useful for the analysis of intact virions by quite a number of laboratories (see e.g. (Bacher et al., 2001; Guha et al., 2012; Havlik et al., 2014; Hogan et al., 2006; Pease, 2012; Thomas et al., 2004; Wick, 2015; Wick and McCubbin, 1999)). In contrast to the CE-UV measurements, the results of nES GEMMA estimated the concentration of the contaminating material rather close to the concentration of RV-A2. This is in agreement with the ratio between viral particles and the amorphous masses observed in negative stain TEM (Weiss et al., 2012).

A fortuitously obtained sample strongly enriched in the contaminant allowed its characterization via CE-UV and nES GEMMA, as well as its confirmation as the popcorn-shaped masses in negative-stain TEM (Weiss et al., 2012). Based on the above observations we suspect that it is a heterogeneous, polydisperse mixture of membranous material, possibly derived from exosomes, since lipase treatment led to its partial disappearance (Weiss et al., 2015a). This latter lipase-treated sample allowed us to finally prepare highly pure empty capsids to determine their M_r via native electrospray ionization mass spectrometry (native ESI MS). The results were in excellent accordance with values calculated from the sum of the building blocks, i.e. 60 copies each of VP1, VP2 and VP3 – note that native virus contains, in addition, 60 copies of VP4 and the genomic RNA of about 7200 to 7300 bases in length (the variation is due to the heterogeneous length of the 3'-poly (A) tail; (Weiss et al., 2015a)). Nevertheless, the purity of our virus preparations was still variable despite lipase treatment (Weiss et al., 2016). This prompted us to assess the utility of anion exchange chromatography (AEX) on a monolithic column for virus purification. AEX was reported to aid for instance the purification of the rod-shaped tomato mosaic virus, hepatitis A virus, calicivirus, PRD1 phage, mumps and measles virus and another picornavirus (enterovirus 71) even leading to a considerable increase of virus concentration in the column eluates (Kovac et al., 2009; Kramberger et al., 2004; Oksanen et al., 2012; Sviben et al., 2017; Venkatachalam et al., 2014). In the following, we demonstrate that AEX also yields a pure RV-A2 fraction well separated from other non-viral components, including ferritin and proteasomes, and free of the ‘contaminant’ as shown by negative stain TEM and nES GEMMA. MALDI mass spectrometry was used to confirm the presence of RV-A2 in the main AEX fraction.

2. Materials and methods

2.1. Chemicals and reagents

Dithiothreitol (DTT, BioUltra), 2-mercaptoethanol (> 98%), iodoacetamide (BioUltra), trifluoroacetic acid (TFA, > 99%), potassium ferricyanide (III) (approx. 99%), tris(hydroxymethyl)aminomethane, sodium chloride, magnesium chloride hexahydrate (Bioreagent), ammonium acetate (NH_4OAc , 99.99% trace metal basis) and ammonium hydroxide (28.2% NH_3) for pH adjustment of NH_4OAc were purchased from Sigma Aldrich (Steinheim, Germany). Ammonium hydrogen carbonate (NH_4HCO_3 , > 99.5%) was obtained from Fluka (Buchs, Switzerland). Acetonitrile (ACN, for analysis, *p.a.*) and formic acid (*p.a.*) were purchased from Merck (Darmstadt, Germany), sodium thiosulfate pentahydrate (*p.a.*) from Riedel-de Haen (Seelze, Germany), trypsin/LysC (MassSpec grade) from Promega (Madison, WI, USA), RNase and DNase from Roche (Mannheim, Germany), trypsin from Life Technologies (Carlsbad, CA, USA). Water used in this study was prepared by means of a Millipore (Billerica, MA, USA) apparatus (18.2 M Ω cm resistivity at 25 °C). Sucrose was obtained from Carl Roth (Karlsruhe, Germany). L-glutamine (2 mM in total from Gibco, Grand Island, NY, USA), Pen-Strep (100 U/mL penicillin, 100 $\mu\text{g}/\text{mL}$ streptomycin in total from Lonza, Verviers, Belgium) and heat inactivated FCS (10% in total from Sigma Aldrich) were supplemented to the cell growth medium.

2.2. RV-A2 preparation

RV-A2 was purified following the protocol detailed in 2015 (Weiss et al., 2015b). In brief, HeLa-H1 cells grown in four 3 L spinner flasks to about 1×10^6 cells/mL were resuspended in fresh SMEM (Sigma Aldrich), adjusted to 2 mM MgCl_2 and supplemented with 2% horse serum (Gibco), infected at $\text{MOI} = 1$, and stirred with 15 rpm at 34 °C for 16.5 h. The low MOI and long incubation time results in two consecutive infection cycles with the first one producing sufficient progeny virus for all cells to become infected in the second round. The conditions were chosen such that the majority of the cells are not yet lysed. They were thus broken with a tight-fitting Dounce homogenizer to set free the intracellular virus. Cell debris was removed by low speed centrifugation and virus in the supernatant was pelleted at 8.0×10^4 g for 2 h in a Ti45 Beckman rotor (Brea, CA, USA) at 4 °C. The pellets were resuspended in 4 mL 20 mM Tris-HCl (pH 7.5), 10 mM EDTA (Merck), and contaminating nucleic acids as well as proteins were digested with DNase and RNase-A (10 min each at ambient temperature) followed by trypsin (5 min at 37 °C). N-laurylsarcosine (Sigma Aldrich) was added for overnight incubation at 4 °C. Aggregated material was removed in an Eppendorf benchtop centrifuge at full speed for 15 min and the supernatant was layered on top of four sucrose density gradients (7.5–45% [w:w]) in 20 mM Tris-HCl (pH 7.4) including 2 mM magnesium chloride prepared in SW40 clear centrifuge tubes (Beckman Coulter). Centrifugation was for 2 h at 1.5×10^5 g at 4 °C. Two turbid bands were visually identified with the more intense one in the middle of the tube and a less intense one in the upper third of the tube. This latter one was brownish, which originates from cellular ferritin as identified by mass spectrometry (data not shown). Both bands were recovered separately with a syringe by perforating the tube. After dilution with 20 mM Tris-HCl (pH 7.4) including 2 mM magnesium chloride, virus was pelleted at 1.0×10^5 g overnight at 4 °C. The pellet was suspended in 150 μL 50 mM Tris-HCl (pH 7.4) including 25 mM sodium chloride and aliquots were frozen at -80 °C. The same procedure was employed for the purification of several other viral serotypes. It is of note that for some RV strains an increase in ionic strength in the buffer used for zonal centrifugation was necessary to prevent virus aggregation (Kim et al., 1989). Therefore, the protocol, as given here for RV-A2, probably needs to be modified to suit different virus strains.

2.3. Monolithic AEX chromatography

For further virus purification, a CIM 1 mL-monolithic diethyl amine (DEAE) column (BIA Separations, Ajdovščina, Slovenia) was selected and equilibrated according to the manufacturer's protocol using 50 mM Tris-HCl (pH 7.4) including 25 mM sodium chloride. The same buffer was used for analyte binding. RV-A2 preparations were brought to a final volume of 1 mL by addition of binding buffer followed by removal of insoluble material via centrifugation (10 min at 2.0×10^4 g at 4 °C). The obtained supernatant was loaded on the column. The chromatography was carried out on an ÄKTA instrument (ÄKTA FPLC, GE Healthcare, Little Chalfont, United Kingdom) at room temperature and a flow rate of 5 mL/min. Unbound material was removed with 15–30 mL binding buffer and finally the sample eluted by applying a linear salt gradient (25 mM to 1 M NaCl in 50 mM Tris-HCl (pH 7.4)) for 10 min. During all chromatographic steps 1 mL fraction were collected. Fractions showing UV absorbance at 280 nm were centrifuged at 1.0×10^5 g overnight and the pellets were suspended in 50 μ L binding buffer. All buffers were filtered through 0.22 μ m membrane filters prior to use.

2.4. TCID₅₀/mL measurements

HeLa cells (HeLa Ohio) were grown in 96 well plates to 40–50% confluency (overnight at 37 °C) in MEM (Life Technologies, Grand Island, NY, USA) supplemented with 30 mM magnesium chloride, 1% L-glutamine, 1% Pen-Strep and 2% heat inactivated FCS. Subsequently, cells were challenged with serially tenfold diluted virus followed by incubation for five days at 34 °C. Cells were stained with 1% crystal violet (Sigma Aldrich) to assess cell viability. Virus titre was determined as 50% tissue culture infectious dose (TCID₅₀/mL), calculated according to the method of Reed and Muench (Reed and Muench, 1938).

2.5. SDS-PAGE

SDS-PAGE was performed by means of 10–20% Tricine gels employing Tricine running buffer diluted from a 10-fold stock (Invitrogen, Carlsbad, CA, USA). SeeBlue Plus2 Pre-stained Protein Standard (Invitrogen) was employed as protein molecular weight marker mix. One μ L RV-A2 (approx. 3 μ g) was mixed with 5 μ L of 2x Tricine SDS sample buffer (Invitrogen) and 4 μ L of water, made 5% 2-mercaptoethanol and heated for 5 min to 95 °C prior to loading onto the gel. SDS-PAGE was performed at 125 mA for 75 min. For assessment of contaminating proteins, the gels were subjected to high-sensitivity, MS-compatible silver-staining (Shevchenko et al., 1996).

2.6. nES GEMMA

nES GEMMA measurements were on a TSI Inc instrument combination (Shoreview, MN, USA) consisting of an nES aerosol generator (Model 3480) equipped with a ^{210}Po α -particle source, a classifier (Model 3080) containing a nano differential mobility analyzer and a butanol-based ultrafine condensation particle counter (Model 3025A). The tipped capillary employed for sample introduction was prepared from a fused silica capillary (40 μ m inner diameter, Polymicro, obtained via Optronis, Kehl, Germany) by application of a home-built grinding machine similar to the setup described by Tycova et al. (Tycova et al., 2016). The instrument was operated under conditions leading to a stable Taylor cone: 4.0 pounds per square inch differential (psid, approx. 28 kPa) and approx. 1.9 kV resulting in currents in the range of –360 nA for sample introduction to the nES. Gas flow, for transport of the nanodroplets through the neutralization chamber and to the size analyzer, was 0.1 L/min (Lpm) CO₂ and 1.0 Lpm compressed, dried (Donaldson Variodry Membrane Dryer Superplus obtained via R. Ludvik Industriegeräte, Vienna, Austria) particle-free air. Individual measurements were carried out between 1.95 and 64.9 nm

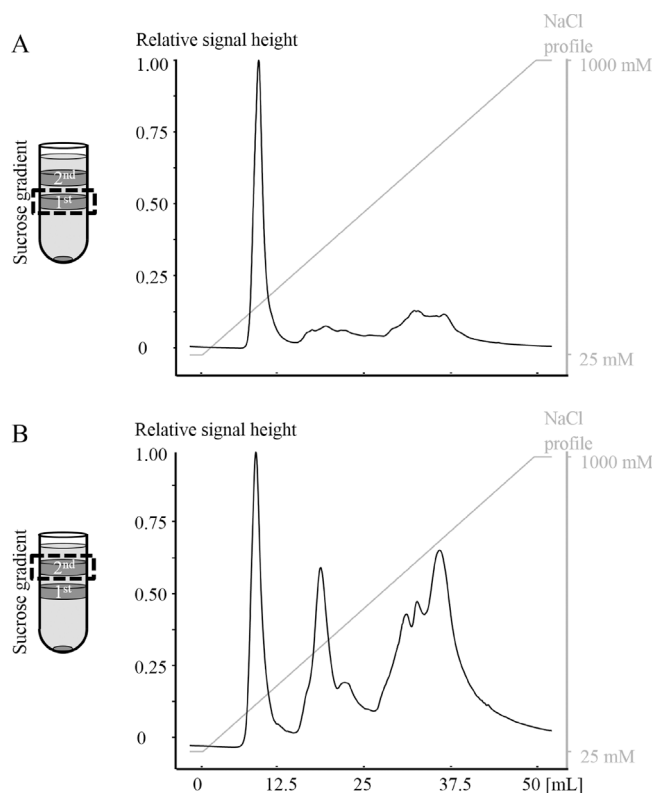


Fig. 1. AEX chromatogram of virus-containing bands recovered from sucrose density gradient centrifugation. ‘First fraction’ (i.e. the band in the middle of the gradient, see inset; A) and ‘second fraction’ (i.e. the band in the upper third of the gradient, see inset; B) were applied onto the column and bound material was eluted with a salt gradient as indicated. Signals ([mAU] at 280 nm UV absorption) were aligned with respect to the relative peak height (y-axis) and the sodium chloride gradient (x-axis) to allow for better comparison of the chromatograms. Note that a small amount of UV-active material was eluted in the flow-through, which is not displayed in the Figure as mentioned in the text.

EM diameter via application of 15 Lpm sheath flow inside the size analyzer. The nES GEMMA spectra depicted were derived from the median of seven respective measurements (100 s scan time, 20 s to reset the high voltage of the size analyzer). Raw particle counts per detector channel are shown, omitting various corrections of the MacroIMS software (version 2.0.1.0.), like for the charge distribution in dependence of nanoparticle size, which especially influences the quantitation of sample components below 10 nm EM diameter. AEX fractions were desalted with 10 kDa molecular weight cutoff centrifugal filters (modified PES membrane from VWR, Vienna, Austria) according to a standard protocol (Weiss et al., 2013). In brief, samples, diluted 1:500 [v:v] in NH₄OAc (40 mM, pH 8.4, filtered through a 0.2 μ m syringe filter), were applied to the filter and the retentate washed once with NH₄OAc after the initial centrifugation step. With respect to the original sample, the finally recovered analytes were diluted 1:60 [v:v] prior to analysis.

2.7. TEM imaging

TEM imaging was done as previously described (Weiss et al., 2015b). Briefly, aliquots of the respective fractions were diluted 1:20 in binding buffer, deposited on Gilder G400 Cu/Pd-grids (Grantham, UK) with a 4.5 nm thick carbon film (glow discharged in a Bal-Tec SCD Sputter Coater (20 mA, 30 s; Scotia, NY, USA)) and stained with 2% uranyl acetate (Electron Microscopy Sciences, Hatfield, PA, USA). Images of the samples were taken with a FEI Morgagni 268D equipped with an 11 megapixel CCD camera (Morada from Olympus-SIS, Muenster, Germany) at 4.4×10^4 fold magnification (80 kV).

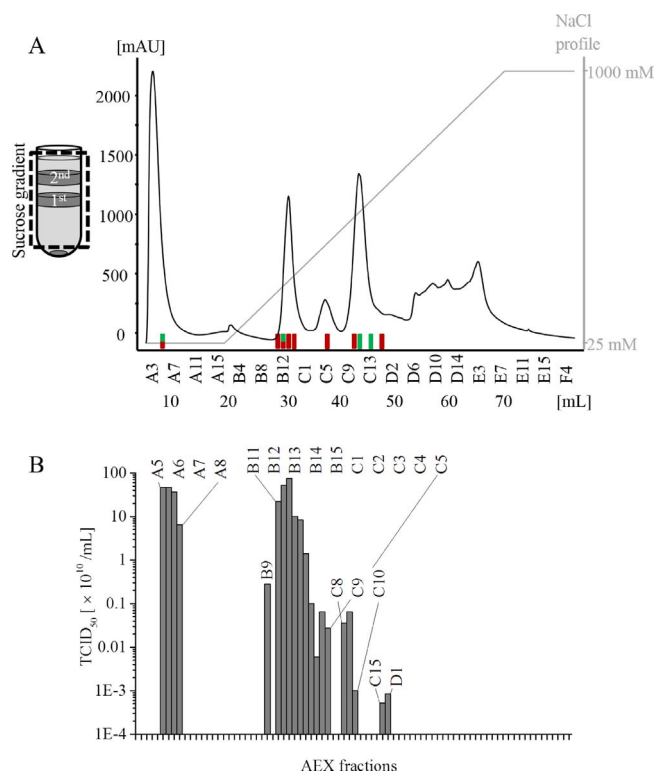


Fig. 2. AEX chromatogram of a RV-A2 preparation. Material recovered from sucrose density gradient centrifugation (with exception of the precipitate, see inset) was separated via AEX chromatography (A). In contrast to Fig. 1 the flow-through was substantial and is, therefore, depicted. The indicated fractions were analyzed via TEM (green) and nES GEMMA (red). Additionally, the viral titer of selected AEX fractions was determined by TCID₅₀ (B). Note that most of the infectious virus particles were found in the flow-through and in the fractions eluting at approx. 200 mM sodium chloride. (For interpretation of the references to colour in this figure legend, the reader is referred to the web version of this article.)

2.8. MALDI MS measurements

After SDS-PAGE, the silver-stained protein bands were excised from the gel and destained with a 1:1 [v:v] mixture of 100 mM sodium thiosulfate and 30 mM potassium ferricyanide (III). Following reduction (10 mM DTT in 100 mM NH₄HCO₃, pH 8.4 at 56 °C for 45 min) and alkylation (54 mM iodoacetamide in 100 mM NH₄HCO₃, pH 8.4 at

room temperature for 30 min under light protection), the proteins were digested at 37 °C overnight with trypsin/LysC in 50 mM NH₄HCO₃, pH 8.4. Tryptic peptides were extracted once with water: ACN (1:1, [v:v]) and twice with formic acid (5%): ACN (1:1, [v:v]). Extracts were combined, dried in vacuo, dissolved in 20 µL of 0.1% aqueous TFA, and desalted by means of C₁₈ Zip Tips (Millipore, Billerica, MA, USA) pre-wetted with ACN (three times). Bound peptides were washed with 0.1% TFA three times followed by elution with 1 µL 0.1% TFA: ACN (1:1, [v:v]) on pre-spotted 1.5 mg/mL α-cyano-4-hydroxycinnamic acid on an AnchorChip MALDI MS target (Bruker, Billerica, MA, USA). MALDI MS measurements were carried out on an UltrafleXtreme (Bruker) in the positive reflectron mode in the *m/z* range of 500–3500 (35–45% laser power for PMF measurements, 50–60% laser power for MS/MS (PSD) experiments).

3. Results and discussion

Numerous preparation and purification protocols for picornaviruses have been published [e.g. (Twomey et al., 1995; Wu et al., 2015)]. They essentially involve a) disruption of the infected cells to release intracellularly accumulated virus progeny, b) differential centrifugation/ultracentrifugation for removing debris and pelleting the virus, c) digestion of contaminating RNA, DNA, and proteins in the presence of a mild detergent, d) velocity and/or equilibrium density gradient ultracentrifugation for banding the virus, and, e) recovery of the virus band followed by pelleting and resuspension of the material in a suitable buffer. In our case, two well-separated turbid bands containing viral material were recovered separately from the sucrose density gradients. The upper band usually contained less infectious virus particles than the lower band and – as revealed by SDS-PAGE – included substantial amounts of virus-unrelated proteins. Furthermore, CE showed a broad peak of unknown nature, which we called the ‘contaminant’. In the lower band, no virus-unrelated material was detected on SDS-PAGE gels stained with Coomassie Brilliant Blue but its presence, in smaller amounts than in the upper band, was revealed by other analytical techniques, including gas-phase electrophoresis (Weiss et al., 2012). Based on its appearance in negative-stain TEM, as well as its susceptibility to lipase digestion, we assumed that this contaminant corresponds to membranous material, possibly exosomes. Therefore, we included a lipase digestion step for its removal (Weiss et al., 2015a). However, the results were variable and preparations devoid of contamination were not obtained in all cases (Weiss et al., 2016). We thus assessed the utility of AEX on a monolithic column as a final purification/polishing step as monoliths have shown in the past their capability

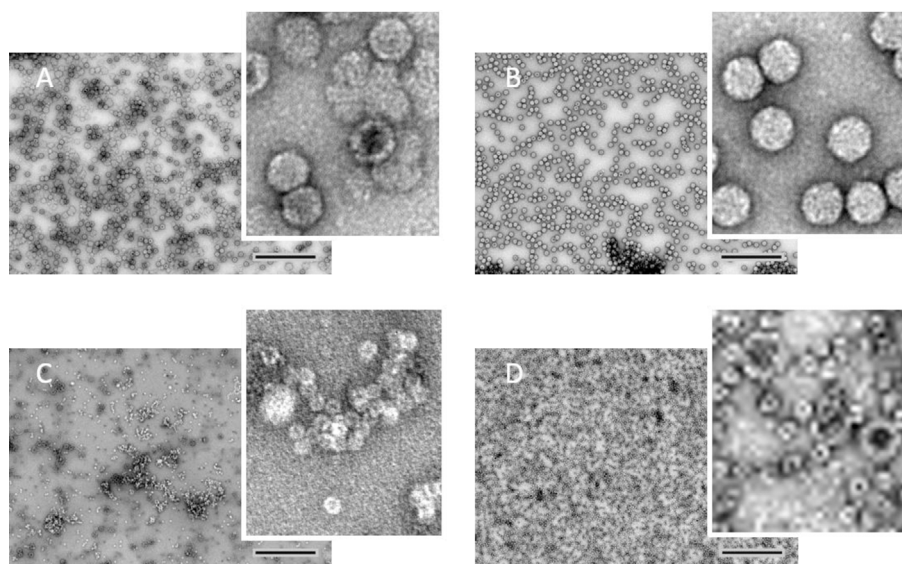


Fig. 3. TEM images of AEX chromatographic fractions as indicated in Fig. 2. Viral particles were detected in fraction A5 (together with the cloud-shaped contaminant, A) and in fraction B12 (B). Fractions C11 (C) and C13 (D) show small spherical particles with approx. 12 nm diameter and rods of approx. 12 × 16 nm dimensions, presumably representing ferritin (Lawson et al., 1991) and proteasomes as inferred from their typical shape (Morimoto et al., 1995). The size bar corresponds to 300 nm. Insets are tenfold magnified with respect to the Figures.

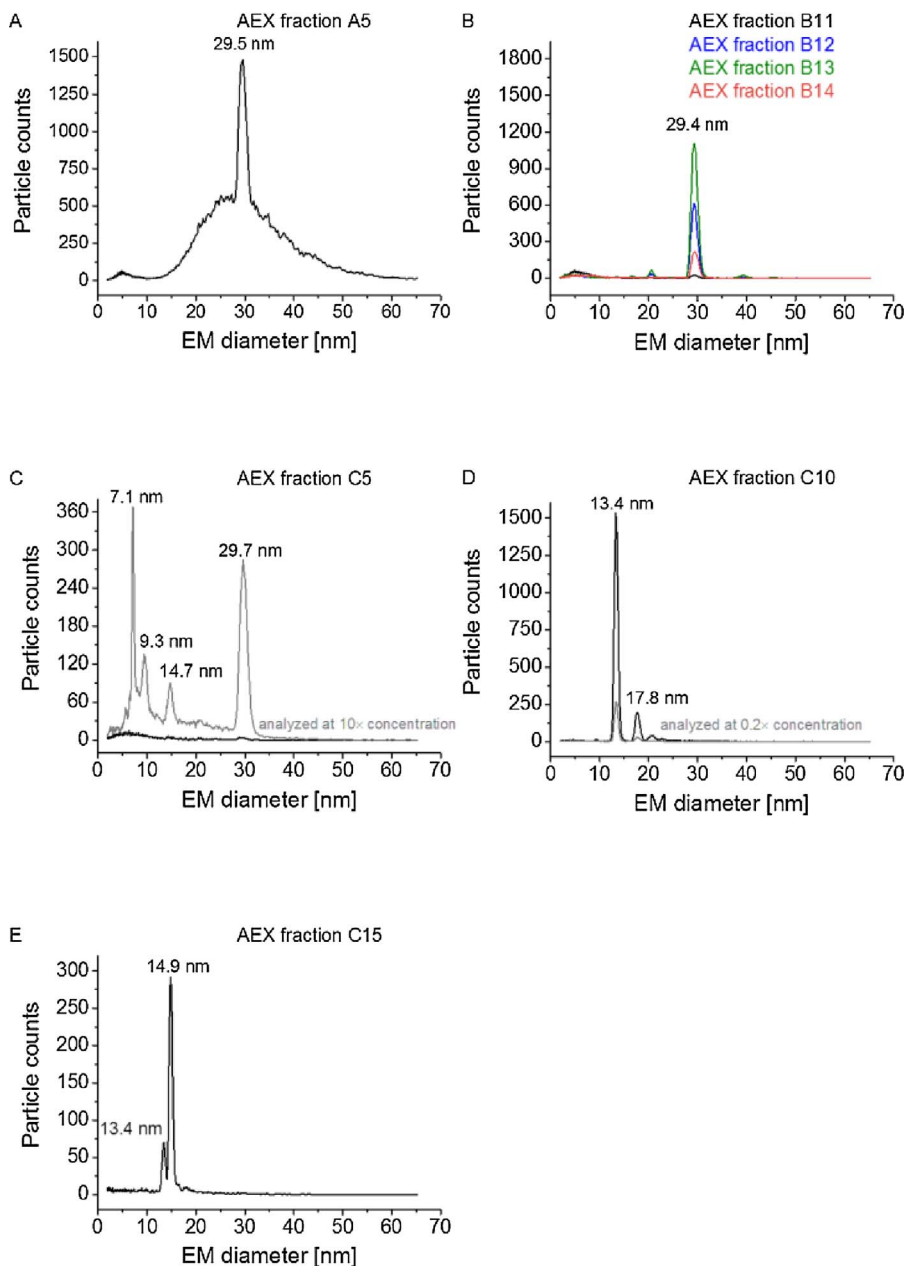


Fig. 4. nES GEMMA spectra of AEX chromatographic fractions indicated in Fig. 2. RV-A2 was detected in fraction A5 – the likewise present contaminant corresponds to the broad, heterogeneous peak between 15 and 50 nm EM diameter – (A), in fractions B11 to B14 (B) and to a significantly lower amount in fraction C5 (besides material with EM diameters below 20 nm, C). The RV-A2 diameter was determined to be 29.5 ± 0.1 nm ($n = 6$ from fractions A5, B11–B14 and C5). Fractions C10 (D) and C13 (E) show particles with EM diameters well below that value.

for purification of macromolecular species such as large protein complexes and viruses.

3.1. Anion exchange chromatography of RV-2 preparations

Apart from RV-A2, we already purified a number of different serotypes such as RV-B14, RV-A16, and RV-A89, using our established standard protocols. In all cases, the same two turbid bands described above were present after sucrose density gradient centrifugation albeit in different proportions. SDS-PAGE usually showed that the lower band was mostly devoid of foreign proteins whereas the upper band was clearly contaminated with non-viral proteins (see reference for RV-A2 (Weiss et al., 2015b)). Separately applying an aliquot of each of the two bands, as obtained from a standard RV-A2 preparation, to an AEX column followed by elution with a sodium chloride gradient (25 mmol/L–1000 mmol/L) resulted in the respective A_{280} extinction profiles shown in Fig. 1A and B. These profiles nicely reflect the different ratios of the main peak, containing the virus eluting at approx. 200 mM sodium chloride, and additional non-virus and UV-absorbing material

eluting later (for confirmation of the identity of the virus see below). The ratio between virus and the additional material was high in the lower band recovered from the sucrose density gradient (Fig. 1A) but much lower in the upper band (Fig. 1B). Note that the absolute signal height values in Fig. 1B were 3.5 fold higher than in Fig. 1A; therefore, relative data were plotted for better comparison of the peak shapes.

As both bands from the sucrose density gradient contained considerable amounts of RV-A2 and because AEX purification appeared to work well even in the presence of large amounts of contaminating compounds (Fig. 1B), we combined in the next step all material after sucrose gradient centrifugation (except the pellet) and subjected the mixture to AEX. This yielded a chromatographic profile (Fig. 2A) very similar to that obtained from the upper band alone (Fig. 1B). It is of note that a substantial amount of material eluted in the column flow-through (depicted in Fig. 2A but not shown in Fig. 1). The quantity of this unbound material varied significantly between various preparations. Subsequent experiments showed that the unbound material also contained RV-A2. We currently ignore the reason for virus eluting in two peaks; it is clearly not related to the column capacity as tested with

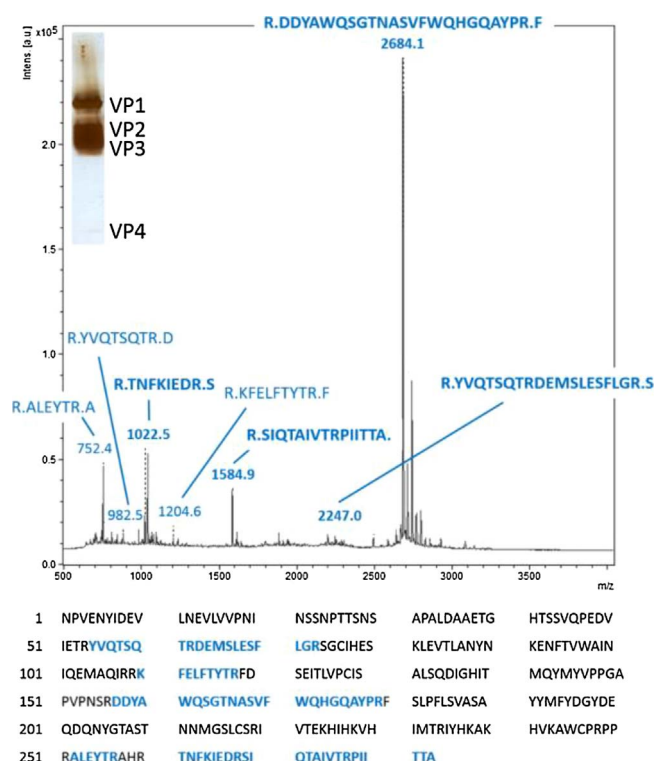


Fig. 5. MALDI MS analysis (peptide mass map) of a sample obtained from AEX chromatographic fraction B14. An aliquot of AEX fraction B14 was subjected to SDS-PAGE with silver staining (inset). Excised bands were subjected to tryptic digestion and analyzed by MALDI MS. The positive ion reflectron mass spectrum for digested VP1 is shown. Several peptides were assigned as indicated. Where MS/MS spectra could be obtained, their sequences are printed in bold; the sequence coverage for VP1 is indicated.

large amounts of bovine serum albumin and RV-A2 on a column with ten-fold higher capacity (data not shown). The bound and unbound virus might correspond to two different conformations of infectious virus similar to the different forms of echovirus recently reported by the group of Marjomaki (Myllynen et al., 2016). Alternatively, differences in the saturation of virus capsids with pocket factor (Oliveira et al., 1993), particle maturation, a so far unexplored microheterogeneity or virus adsorption to the chromatographic material via a ‘bridging’ component present in the sample might account for our finding.

To determine the distribution of infectious viral particles, selected AEX fractions were subjected to TCID₅₀ assays. Infectivity was highest in the flow-through and in the fractions eluting at approx. 200 mM sodium chloride (Fig. 2B). In the above context it is rather striking to mention that material initially eluting in the flow-through behaved virtually identically when re-subjected to AEX separation. However, the virus eluting at approx. 200 mM sodium chloride was only partially retained on the column upon repeated injection suggesting that its interaction with the stationary phase had changed.

3.2. Nature of RV-A2 in the AEX fractions

Aliquots of AEX peak fractions (green in Fig. 2A) were examined by TEM (Fig. 3). Material in the flow-through contained virions as well as empty capsids (the latter probably an artefact resulting from interaction with the carbon coating of the grid and/or the staining process) together with particles with the typical morphology of the contaminant (Fig. 3A). The peak, eluting at approx. 200 mM sodium chloride was virtually pure virus (Fig. 3B). Material eluting at higher ionic strength included broken subviral particles that had lost their RNA genome and a high proportion of either ferritin (Fig. 3C) or particles tentatively identified as proteasomes from their typical shape (Fig. 3D). Both fractions also contained some virus particles or empty capsids, albeit at

significantly lower concentration than in fractions A5 and B12.

nES GEMMA measurements (Fig. 4A–E) of similar AEX fractions (indicated in red in Fig. 2A) led to the same conclusion. The flow-through contained virus together with substantial amounts of the contaminant (Fig. 4A) whereas highly-pure RV-A2 was found in fractions of the peak eluting at approx. 200 mM sodium chloride (Fig. 4B). AEX fraction C5 (Fig. 4C) likewise contained some RV-A2, yet at a significantly lower concentration.

Subjecting other AEX fractions to TEM and nES GEMMA analysis allowed a first characterization of additional sample components. nES GEMMA yielded EM diameter values of 13.4 nm and 14.9 nm for the main components detected in fractions C10 and C15 (Fig. 4D and E). Correlating these EM diameters with relative molecular weights of protein complexes (e.g. Bacher et al., 2001) lead to approx. M_r values of 434 and 602 kDa. A M_r of 434 kDa, as found for the main component in fraction C10 (Fig. 4D), is in good accordance with the theoretically predicted and experimentally found value of ferritin. The faint reddish color together with the small spherical morphology and high electron density observed in TEM (Fig. 3C) is in favor of this assumption. On the other hand, in accordance with the typical rod-like morphology seen in the TEM image (Fig. 3D), the material in fraction C13 might be 20S proteasomes with a M_r of 700 kDa (Coux et al., 1996) and fragments thereof.

3.3. MALDI mass spectrometric confirmation of RV-A2 in the AEX main fraction

Intact virions were detected in the AEX flow-through as well as in fractions eluting at approx. 200 mM sodium chloride as identified by TEM and nES GEMMA measurements. As desired, the latter samples were of significantly higher purity. Therefore, an aliquot of an exemplary fraction (B14) was subjected to virus identification via SDS-PAGE followed by enzymatic digestion of the protein bands and MALDI MS measurement. We obtained a significant score for VP1 with a sequence coverage of 28% as shown in Fig. 5. MS/MS experiments of several detected peptides confirmed this identification. Similar results were obtained for VP2. Insufficient separation of VP2 and VP3 on the SDS-PAGE gel resulted in ambiguous identification of VP3. Finally, the faint, low molecular mass band corresponding potentially to VP4 was not available in sufficient amount for identification. Nevertheless, MALDI MS allowed for unequivocal identification of RV-A2 in AEX fraction B14 and hence (together with TEM, nES GEMMA, and SDS-PAGE) for identification as material mainly comprising the chromatographic peak eluting at approx. 200 mM sodium chloride from the monolithic column.

4. Conclusion

Homogeneous preparations of infectious viruses without contaminating components are a necessary prerequisite to address questions of biological, immunological, and bioanalytical relevance. Monolithic AEX chromatography as additional purification or polishing step significantly improved the purity of rhinoviruses exemplified by RV-A2 as demonstrated via TEM and nES GEMMA measurements while preserving its infectivity. However, we observed that only a fraction of the initial virus material was bound to the stationary phase and could be eluted with a sodium chloride gradient yielding virus of high purity. Identity of this material was confirmed by SDS-PAGE with high sensitivity silver staining followed by MALDI MS. Clarification of why a part of RV-A2 was not retained on the column and why the retained virus converted partly into non-retained virus is currently being addressed. Loading experiments excluded saturation of the AEX column. Possible reasons for this phenomenon might be different degrees of saturation with pocket factor (Oliveira et al., 1993), so far unexplored microheterogeneity, virus particle maturation, or adsorbing to the chromatographic material via a ‘bridging’ compound. Indeed, the fact that once

bound virus partially eluted in the flow-through upon re-injection into the AEX column might point to the latter possibility or indicate structural changes impinged on the virus particle by interactions with the matrix. In fact, it has been observed that adsorption to polymeric material might lead to tertiary/quaternary structural changes of proteins (Ballet et al., 2010). Nevertheless, despite these unanswered questions our method yields high-purity viral preparations. This is a significant step forward in rhinovirus research.

Acknowledgements

This project was supported by Austrian Science Fund (FWF) grants P27444 (to DB), P27196 (to HK) and P25749-B20 (to VUW).

References

- Ashley, C.R., Caul, E.O., 1982. Potassium tartrate-glycerol as a density gradient substrate for separation of small, round viruses from human feces. *J. Clin. Microbiol.* 16, 377–381.
- Bacher, G., Szymanski, W.W., Kaufman, S.L., Zollner, P., Blaas, D., Allmaier, G., 2001. Charge-reduced nano electrospray ionization combined with differential mobility analysis of peptides, proteins, glycoproteins, noncovalent protein complexes and viruses. *J. Mass Spectrom.* 36, 1038–1052.
- Ballet, T., Boulange, L., Brechet, Y., Bruckert, F., Weidenhaupt, M., 2010. Protein conformational changes induced by adsorption onto material surfaces: an important issue for biomedical applications of material science. *Bull. Pol. Acad. Tech.* 58, 303–315.
- Bilek, G., Weiss, V.U., Pickl-Herk, A., Blaas, D., Kenndler, E., 2009. Chip electrophoretic characterization of liposomes with biological lipid composition: coming closer to a model for viral infection. *Electrophoresis* 30, 4292–4299.
- Coux, O., Tanaka, K., Goldberg, A.L., 1996. Structure and functions of the 20S and 26S proteasomes. *Annu. Rev. Biochem.* 65, 801–847.
- Gugerli, P., 1984. Isopycnic centrifugation of plant viruses in nycodenz density gradients. *J. Virol. Methods* 9, 249–258.
- Guha, S., Li, M., Tarlov, M.J., Zachariah, M.R., 2012. Electrospray-differential mobility analysis of bionanoparticles. *Trends Biotechnol.* 30, 291–300.
- Havlik, M., Marchetti-Deschmann, M., Friedbacher, G., Messner, P., Winkler, W., Perez-Burgos, L., Tauer, C., Allmaier, G., 2014. Development of a bio-analytical strategy for characterization of vaccine particles combining SEC and nanoES GEMMA. *Analyst* 139, 1412–1419.
- Hogan Jr., C.J., Kettleson, E.M., Ramaswami, B., Chen, D.R., Biswas, P., 2006. Charge reduced electrospray size spectrometry of mega- and gigadalton complexes: whole viruses and virus fragments. *Anal. Chem.* 78, 844–852.
- Kaufman, S.L., Skogen, J.W., Dorman, F.D., Zarrin, F., Lewis, K.C., 1996. Macromolecule analysis based on electrophoretic mobility in air: globular proteins. *Anal. Chem.* 68, 1895–1904.
- Kim, S.S., Smith, T.J., Chapman, M.S., Rossmann, M.C., Pevear, D.C., Dutko, F.J., Felock, P.J., Diana, G.D., McKinlay, M.A., 1989. Crystal structure of human rhinovirus serotype 1A (HRV1A). *J. Mol. Biol.* 210, 91–111.
- Kolivoska, V., Weiss, V.U., Kremser, L., Gas, B., Blaas, D., Kenndler, E., 2007. Electrophoresis on a microfluidic chip for analysis of fluorescence-labeled human rhinovirus. *Electrophoresis* 28, 4734–4740.
- Kovac, K., Gutierrez-Aguirre, I., Banjac, M., Peterka, M., Poljsak-Prijatelj, M., Ravnikar, M., Mijovski, J.Z., Schultz, A.C., Raspor, P., 2009. A novel method for concentrating hepatitis A virus and caliciviruses from bottled water. *J. Virol. Methods* 162, 272–275.
- Kramberger, P., Petrovic, N., Strancar, A., Ravnikar, M., 2004. Concentration of plant viruses using monolithic chromatographic supports. *J. Virol. Methods* 120, 51–57.
- Kremser, L., Konecni, T., Blaas, D., Kenndler, E., 2004. Fluorescence labeling of human rhinovirus capsid and analysis by capillary electrophoresis. *Anal. Chem.* 76, 4175–4181.
- Kremser, L., Petsch, M., Blaas, D., Kenndler, E., 2006. Influence of detergent additives on mobility of native and subviral rhinovirus particles in capillary electrophoresis. *Electrophoresis* 27, 1112–1121.
- Lawson, D.M., Artymiuk, P.J., Yewdall, S.J., Smith, J.M., Livingstone, J.C., Treffry, A., Luzzago, A., Levi, S., Arosio, P., Cesareni, G., et al., 1991. Solving the structure of human H ferritin by genetically engineering intermolecular crystal contacts. *Nature* 349, 541–544.
- Liu, C.C., Guo, M.S., Lin, F.H., Hsiao, K.N., Chang, K.H., Chou, A.H., Wang, Y.C., Chen, Y.C., Yang, C.S., Chong, P.C., 2011. Purification and characterization of enterovirus 71 viral particles produced from vero cells grown in a serum-free microcarrier bioreactor system. *PLoS One* 6, e20005.
- Morimoto, Y., Mizushima, T., Yagi, A., Tanahashi, N., Tanaka, K., Ichihara, A., Tsukihara, T., 1995. Ordered structure of the crystallized bovine 20S proteasome. *J. Biochem.* 117, 471–474.
- Myllynen, M., Kazmertsuk, A., Marjomaki, V., 2016. A novel open and infectious form of echovirus 1. *J. Virol.* 90, 6759–6770.
- Oksanen, H.M., Domanska, A., Bamford, D.H., 2012. Monolithic ion exchange chromatographic methods for virus purification. *Virology* 434, 271–277.
- Oliveira, M.A., Zhao, R., Lee, W.M., Kremer, M.J., Minor, I., Rueckert, R.R., Diana, G.D., Pevear, D.C., Dutko, F.J., McKinlay, M.A., et al., 1993. The structure of human rhinovirus 16. *Structure* 1, 51–68.
- Pease 3rd, L.F., 2012. Physical analysis of virus particles using electrospray differential mobility analysis. *Trends Biotechnol.* 30, 216–224.
- Reed, L.J., Muench, H., 1938. A simple method of estimating fifty percent endpoints. *Am. J. Epidemiol.* 27, 493–497.
- Shevchenko, A., Wilm, M., Vorm, O., Mann, M., 1996. Mass spectrometric sequencing of proteins silver-stained polyacrylamide gels. *Anal. Chem.* 68, 850–858.
- Sviben, D., Forcic, D., Ivancic-Jelecki, J., Halassy, B., Brgles, M., 2017. Recovery of infective virus particles in ion-exchange and hydrophobic interaction monolith chromatography is influenced by particle charge and total-to-infective particle ratio. *J. Chromatogr. B* 1054, 10–19.
- Thomas, J.J., Bothner, B., Traina, J., Benner, W.H., Siuzdak, G., 2004. Electrospray ion mobility spectrometry of intact viruses. *Spectroscopy* 18, 31–36.
- Twomey, T., Newman, J., Burrage, T., Piatti, P., Lubroth, J., Brown, F., 1995. Structure and immunogenicity of experimental foot-and-mouth disease and poliomyelitis vaccines. *Vaccine* 13, 1603–1610.
- Tycova, A., Prikyr, J., Foret, F., 2016. Reproducible preparation of nanospray tips for capillary electrophoresis coupled to mass spectrometry using 3D printed grinding device. *Electrophoresis* 37, 924–930.
- Venkatachalam, A.R.K., Szyporta, M., Kiener, T.K., Balraj, P., Kwang, J., 2014. Concentration and purification of enterovirus 71 using a weak anion-exchange monolithic column. *Virol. J.* 11.
- Weiss, V.U., Kolivoska, V., Kremser, L., Gas, B., Blaas, D., Kenndler, E., 2007. Virus analysis by electrophoresis on a microfluidic chip. *J. Chromatogr. B Anal. Technol. Biomed. Life Sci.* 860, 173–179.
- Weiss, V.U., Subirats, X., Pickl-Herk, A., Bilek, G., Winkler, W., Kumar, M., Allmaier, G., Blaas, D., Kenndler, E., 2012. Characterization of rhinovirus subviral A particles via capillary electrophoresis, electron microscopy and gas-phase electrophoretic mobility molecular analysis: part I. *Electrophoresis* 33, 1833–1841.
- Weiss, V.U., Lehner, A., Kerul, L., Grombe, R., Kratzmeier, M., Marchetti-Deschmann, M., Allmaier, G., 2013. Characterization of cross-linked gelatin nanoparticles by electrophoretic techniques in the liquid and the gas phase. *Electrophoresis* 34, 3267–3276.
- Weiss, V.U., Bereszczak, J.Z., Havlik, M., Kallinger, P., Gosler, I., Kumar, M., Blaas, D., Marchetti-Deschmann, M., Heck, A.J., Szymanski, W.W., Allmaier, G., 2015a. Analysis of a common cold virus and its subviral particles by gas-phase electrophoretic mobility molecular analysis and native mass spectrometry. *Anal. Chem.* 87, 8709–8717.
- Weiss, V.U., Subirats, X., Kumar, M., Harutyunyan, S., Gosler, I., Kowalski, H., Blaas, D., 2015b. Capillary electrophoresis, gas-phase electrophoretic mobility molecular analysis, and electron microscopy: effective tools for quality assessment and basic rhinovirus research. *Methods Mol. Biol.* 1221, 101–128.
- Weiss, V.U., Bliem, C., Gosler, I., Fedosyuk, S., Kratzmeier, M., Blaas, D., Allmaier, G., 2016. In vitro RNA release from a human rhinovirus monitored by means of a molecular beacon and chip electrophoresis. *Anal. Bioanal. Chem.* 408, 4209–4217.
- Wick, C.H., McCubbin, P.E., 1999. Characterization of purified MS2 bacteriophage by the physical counting methodology used in the integrated virus detection system (IVDS). *Toxicol. Method* 9, 245–252.
- Wick, C.H., 2015. Integrated Virus Detection. CRC Press, Boca Raton.
- Wu, C.Y., Lin, Y.W., Kuo, C.H., Liu, W.H., Tai, H.F., Pan, C.H., Chen, Y.T., Hsiao, P.W., Chan, C.H., Chang, C.C., Liu, C.C., Chow, Y.H., Chen, J.R., 2015. Inactivated enterovirus 71 vaccine produced by 200-L scale serum-free microcarrier bioreactor system provides cross-protective efficacy in human SCAR2 transgenic mouse. *PLoS One* 10, e0136420.